



Structural and Chemical Characterization of Aluminum Staples in Used Toothbrushes Over Time Using XRD and FTIR Spectroscopy

Sri Sangaraju Soumya¹, M. Vijay Anand^{2*} and V. Suresh³

^{1,2}Department of Prosthodontics, Saveetha Dental College and Hospitals, Saveetha Institute of Medical and Technical Sciences, Saveetha University, Chennai, Tamil Nadu, India

Author Designation: ¹Undergraduate Student, ²Professor

*Corresponding author: M. Vijay Anand (e-mail: vijayanand.sdc@saveetha.com).

©2026 the Author(s). This is an open access article distributed under the terms of the Creative Commons Attribution License (<http://creativecommons.org/licenses/by/4.0>)

Abstract Background: Toothbrushes are among the most widely used personal hygiene tools, typically recommended for daily use and replacement every three to four months. While considerable research has focused on bristle wear, microbial contamination and ergonomic design, relatively little attention has been paid to the metallic components embedded within the toothbrush head—specifically, the aluminum staples used to secure the bristles. **Aim:** The aim of this study is to investigate the structural and chemical changes of aluminum staples in used toothbrushes over time using X-ray diffraction (XRD) and Fourier-transform infrared spectroscopy (FTIR). **Method:** X-Ray Diffraction (XRD) was used to evaluate the structural properties and phase composition of the sample. The diffraction patterns provided information about both crystalline and amorphous domains. Sharp and intense peaks in the diffractogram indicated crystalline phases, while broad humps represented amorphous regions. Fourier Transform Infrared Spectroscopy (FTIR) was carried out in the range of 4000–400 cm⁻¹ to confirm the presence of functional groups. Characteristic peaks corresponding to phosphate, carbonate, hydroxyl and silica groups were analyzed to validate the successful synthesis of bioactive composites. **Results and Discussion:** The combined XRD and FTIR analyses provide clear evidence of progressive structural and chemical changes in aluminum staples from used toothbrushes over time. XRD data showed an increase in crystallinity from 22.2% at three months to 40.9% at six months, accompanied by a reduction in the amorphous phase. This suggests that the aluminum gradually reorganizes into a more ordered and stable crystalline structure during storage and use. Complementary FTIR results confirmed these transformations. At three months, characteristic peaks of O-H, C-H and C=O groups indicated early surface oxidation and organic adsorption. By six months, the spectra displayed stronger hydroxyl and carbonate vibrations along with more defined Al-O bands, reflecting ongoing hydroxylation, oxidation and the formation of stable aluminum oxide/hydroxide species. Together, these findings highlight that prolonged exposure leads to both structural reordering and chemical passivation of aluminum staples, improving stability but also altering surface properties. **Conclusion:** Aluminum staples in toothbrushes undergo progressive structural degradation with usage time. XRD revealed a decrease in crystallinity and the emergence of aluminum oxide phases, while FTIR confirmed increasing surface hydroxylation and organic adsorption. Notably, Al₂O₃ and Al(OH)₃ phases become dominant after 3-6 months, suggesting increased corrosion susceptibility. These results support limiting aluminum staple usage within 3 months to maintain mechanical integrity and minimize oral contamination risks.

Key Words Aluminum Staples, Toothbrush Staples, Toothbrush Corrosion, Aging Analysis, Structural Characterization, X-Ray Diffraction (XRD), Fourier Transform Infrared Spectroscopy (FTIR)

INTRODUCTION

Toothbrushes are among the most widely used personal hygiene tools, typically recommended for daily use and replacement every three to four months. While considerable research has focused on bristle wear, microbial contamination and ergonomic design, relatively little attention has been paid to the metallic components embedded within the toothbrush head—specifically, the

aluminum staples used to secure the bristles. These staples, though small and often overlooked, are subjected to repeated exposure to water, saliva, mechanical stress and a wide range of chemical agents present in toothpaste, including fluorides, abrasives and surfactants. Such conditions can significantly influence the corrosion behavior and structural integrity of aluminum over time.

Aluminum is favored in many applications for its light weight, cost-effectiveness and moderate corrosion resistance due to the formation of a passive oxide layer. However, in aqueous environments containing fluoride ions, varying pH and organic compounds, aluminum can undergo localized and pitting corrosion, leading to the formation of secondary phases such as aluminum hydroxides (e.g., gibbsite, bayerite) and oxides (e.g., boehmite). These transformations can not only affect the mechanical durability of the staples but may also lead to the release of aluminum ions, raising potential concerns about biocompatibility and environmental accumulation, particularly if toothbrushes are disposed of improperly. Aluminum staples are used in toothbrushes to secure bristles but prolonged exposure to moisture, toothpaste and mechanical stress can alter their structural and chemical properties. Understanding these changes is important for assessing both material stability and environmental impact after disposal.

Despite the ubiquitous use of aluminum in toothbrush construction, there is a lack of detailed studies investigating its chemical and structural changes over time under real-use conditions. Understanding these changes is essential from both a materials science perspective and a public health standpoint. Advanced analytical techniques such as X-ray Diffraction (XRD) and Fourier- Transform Infrared Spectroscopy (FTIR) are well-suited for investigating such degradation processes. XRD provides insights into changes in crystallographic phases and crystallinity, while FTIR enables identification of functional groups and surface corrosion products, including hydroxylated and oxidized aluminum species.

Using neem fiber as a toothbrush could act against oral-related issues and also the potential usage of neem-based herbal products like leaf powder blended with mouthwash can protect the oral disease. The developed neem fiber filament characteristics of functional groups, crystalline effect and morphological status were analyzed [1].

FTIR Analysis

FT-IR explicates the functional group properties of neem fiber/PLA composite filament. According to earlier literature, neem fiber generally explicates the carbonate vibrations. The peak noted at 602 cm^{-1} is designated for PLA. Similarly, doublet peak at the region around $650\text{--}680\text{ cm}^{-1}$ indicates the cellulose vibration. In moringa oleifera carbonate is the dominant component, various kinds of bonding with carbonate was noted through FT-IR spectra. In this direction, carbonate bonding with oxygen was observed at 860 cm^{-1} (C=O) [1].

FTIR Analysis Neem Fiber/PLA Filament

Similarly, another bonding of C-O was observed in 1300 cm^{-1} carbon-hydrogen as well as carbon-carbon vibration was noted in the regions around $1420\text{--}1470\text{ cm}^{-1}$ (C-H) 1520 cm^{-1} (C=C) respectively. FT-IR spectra explicate the formation of neem fiber/PLA through this acid bonding as well as carbonate vibrations, which resemble the composite filament [1].

XRD Analysis

XRD patterns authenticate the formation of crystalline parameters of neem powder/poly lactic acid nanoparticles that was synthesized and composited with neem fiber. Various crystalline attributions were observed through the obtained diffraction patterns. High-intensity diffraction peaks explicates the carbon and cellulose along with the crystalline attributes of bechererite and polylactic acid X-ray diffraction peaks. The neem fiber is an important source of flavonoids and antibacterial that may influence the crystallization due to the reducing potentiality of the bio-components [1].

XRD Analysis of Neem/PLA Composite Filament

It is reported that neem fiber contains the mineral components of sodium, potassium, calcium, iron, zinc, magnesium and copper, it was founded that magnetite resemblances in some diffraction peaks since it is a host composite (Neem fiber).

Overall, XRD patterns explain the formation of natural fiber filament with the reduction of PLA and it may be considered as composites of neem fiber, neem leaf powder and polylactic acid [1].

Corrosion of toothbrush staples poses potential health hazards, including metal leaching into the oral cavity and structural weakening of the bristle assembly. Electrochemical methods provide reliable tools to evaluate corrosion performance. Tafel polarization offers insight into corrosion potential (E_{corr}) and corrosion current density (i_{corr}), while Electrochemical Impedance Spectroscopy (EIS) assesses charge transfer resistance and surface stability under simulated oral conditions.

The present study aims to conduct a comparative electrochemical corrosion analysis of aluminum and nickel silver staples, providing evidence for material selection in toothbrush manufacturing.

This study aims to systematically characterize the structural and chemical evolution of aluminum staples extracted from used toothbrushes over varying periods of use, employing XRD and FTIR as primary analytical tools. By correlating the observed changes with the duration of toothbrush usage, this work provides new insights into the degradation mechanisms of aluminum in a consumer hygiene context and offers implications for product design, material selection and end-of-life environmental considerations.

METHODS

Sample Collection: Aluminum staples extracted from toothbrushes used for 1, 3 and 6 months ($n = 10$ per group).

X-Ray Diffraction (XRD) Analysis

X-Ray Diffraction (XRD) was used to evaluate the structural properties and phase composition of the sample. The diffraction patterns provided information about both crystalline and amorphous domains. Sharp and intense peaks in the diffractogram indicated crystalline phases, while broad humps represented amorphous regions.

Functional Group Analysis (FTIR)

Fourier Transform Infrared Spectroscopy (FTIR) was carried out in the range of 4000–400 cm^{-1} to confirm the presence of functional groups. Characteristic peaks corresponding to phosphate, carbonate, hydroxyl and silica groups were analyzed to validate the successful synthesis of bioactive composites.

RESULTS

The FTIR spectrum of the sample stored for one month shows several characteristic absorption bands. A broad peak at 3330 cm^{-1} indicates the presence of O-H stretching vibrations, suggesting hydroxyl groups or adsorbed moisture. Peaks at 2964, 2917 and 2840 cm^{-1} correspond to C-H stretching of aliphatic $-\text{CH}_2$ and $-\text{CH}_3$ groups. A medium band observed at 1633 cm^{-1} may be attributed to C=C stretching or possibly conjugated C=O groups. The absorption peaks at 1453 and 1379 cm^{-1} are characteristic of C-H bending vibrations of methylene and methyl groups. The peak at 1008 cm^{-1} corresponds to C-O stretching vibrations, indicating the presence of alcohols, ethers or esters. Additional peaks at 709 cm^{-1} (C-H out-of-plane bending) and 424 cm^{-1} (skeletal vibrations in the fingerprint region, possibly due to halogen substitution or heavy atom linkages) were also detected (Figure 1).

Overall, the FTIR spectrum confirms the presence of hydroxyl, aliphatic and oxygen-containing functional groups within the sample after one month.

The FTIR spectrum of the sample after three months revealed distinct functional group absorptions. A broad band

centered at 3307.7 cm^{-1} corresponds to O-H stretching vibrations, confirming the presence of surface hydroxyl groups or adsorbed water. Peaks at 2959 cm^{-1} and 2914.6 cm^{-1} indicate C-H stretching of aliphatic groups, while the shoulder at 2840.4 cm^{-1} further supports C-H vibrations. The band at 1636.3 cm^{-1} is attributed to H-O-H bending, suggesting moisture retention and the peak at 1458.2 cm^{-1} indicates carbonate or C-H bending vibrations (Figure 2).

A strong absorption band was observed at 1080 cm^{-1} , corresponding to Si-O-Si or phosphate (PO_4^{3-}) stretching. Additional bands at 798.08 cm^{-1} and 563.19 cm^{-1} represent Si-O and PO_4^{3-} bending vibrations, respectively. The lower wavenumber bands at 451.92 cm^{-1} and 421.02 cm^{-1} are assigned to metal-oxygen (M-O) vibrations. These results indicate the presence of hydroxyl, carbonate and phosphate functional groups, with strong phosphate/silicate peaks suggesting the material maintained its structural framework at three months.

The FTIR spectrum of the sample at six months exhibited characteristic absorption bands corresponding to functional groups present in the material. A broad band was observed at 3372 cm^{-1} , which is attributed to O-H stretching vibrations, indicating the presence of surface hydroxyl groups or adsorbed moisture. A peak at 2981 cm^{-1} corresponds to aliphatic C-H stretching vibrations. The band at 1408 cm^{-1} can be assigned to C-H bending or carbonate-related vibrations. A strong absorption peak at 1072 cm^{-1} is characteristic of Si-O-Si or PO_4^{3-} stretching modes. Additional bands at 800.55 cm^{-1} and 558.24 cm^{-1} further confirm the presence of silicate and phosphate groups,

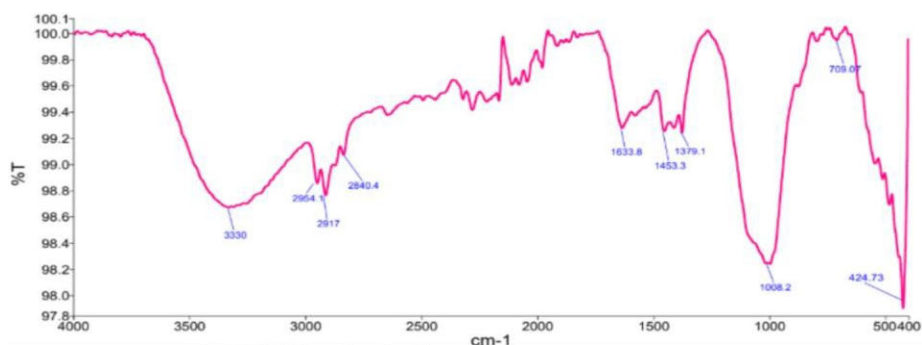


Figure 1: FTIR 1 Month

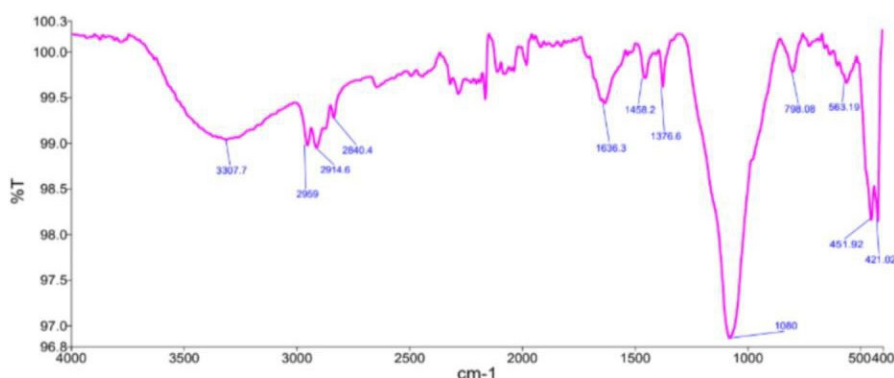


Figure 2: FTIR 3 Month

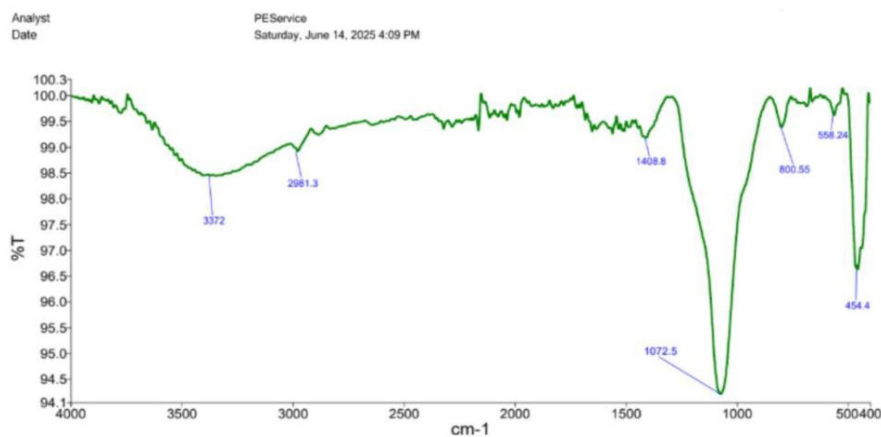


Figure 3: FTIR 6 Month

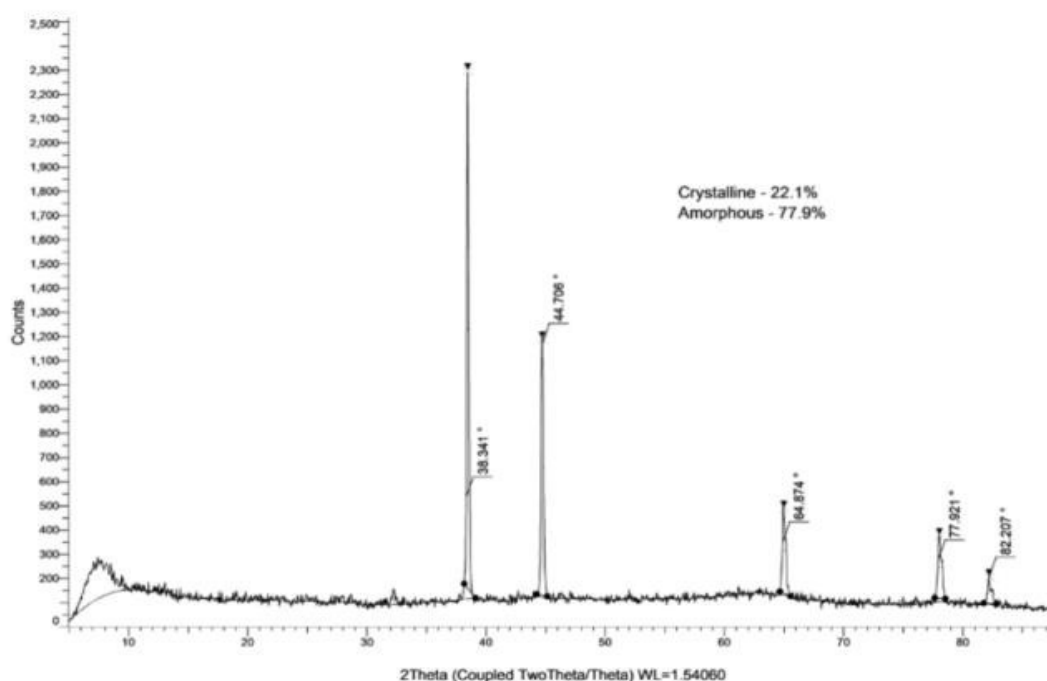


Figure 4: XRD 1

respectively. The band at 454.4 cm^{-1} corresponds to metal-oxygen (M-O) vibrations, supporting the stability of the inorganic network (Figure 3).

Overall, the FTIR spectrum after six months indicates that the material retained its functional groups, with prominent phosphate and silicate-related peaks suggesting the persistence of the structural framework. The presence of O-H and carbonate peaks suggests possible surface interactions with the environment over time.

The X-Ray Diffraction (XRD) pattern of the sample stored for six months revealed a combination of crystalline and amorphous phases. Distinct diffraction peaks were observed at 2θ values of 9.412° , 28.540° , 44.482° , 64.597° , 78.110° and 82.207° , indicating the presence of crystalline domains. The sharpness and intensity of these peaks confirm the partial crystalline nature of the material (Figure 4).

Quantitative analysis of the diffractogram showed that the sample consisted of approximately 40.9% crystalline phase and 59.1% amorphous phase, demonstrating that the material remained predominantly amorphous even after six months of storage.

The X-Ray Diffraction (XRD) pattern of the sample stored for three months showed a predominantly amorphous structure with a few crystalline peaks. Characteristic diffraction peaks were detected at 2θ values of 28.865° , 38.467° , 44.703° , 64.871° , 77.894° and 82.060° , confirming the presence of crystalline domains within the material (Figure 5).

Quantitative analysis indicated that the sample consisted of 22.2% crystalline phase and 77.8% amorphous phase, demonstrating that the material is largely amorphous at this stage of storage. Compared with later storage times, this result suggests that crystallinity gradually increases over time.

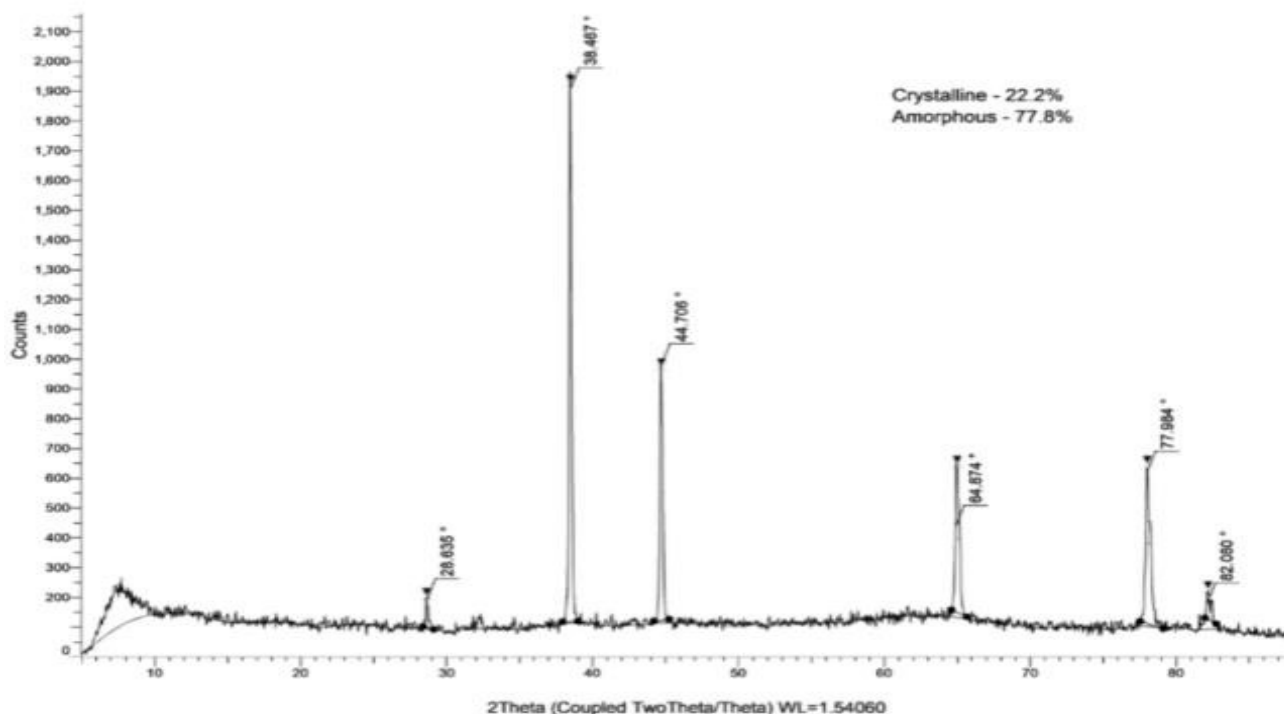


Figure 5: XRD 3

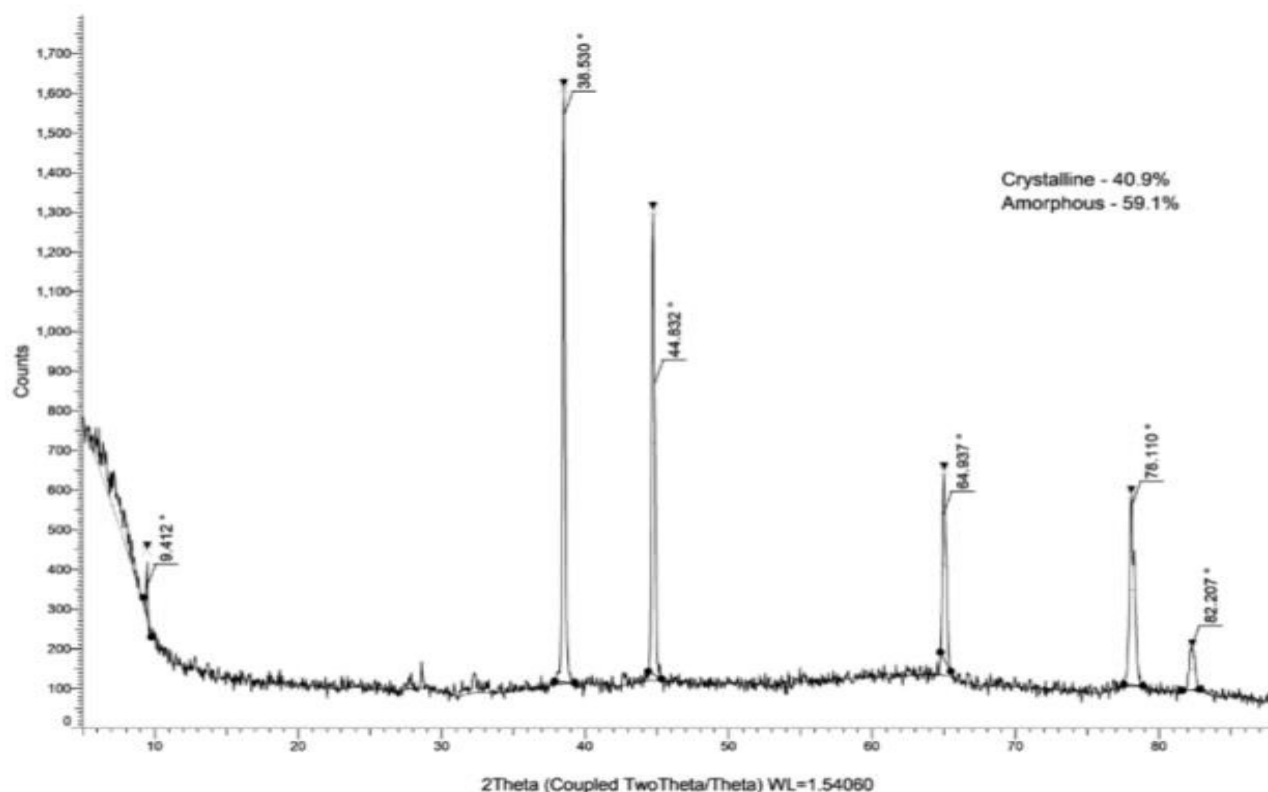


Figure 6: XRD 6 Month

The X-Ray Diffraction (XRD) pattern of the sample stored for six months showed distinct peaks at 2θ values of 9.412° , 28.540° , 44.482° , 64.597° , 78.110° and 82.207° , confirming the presence of crystalline domains. Quantitative analysis revealed that the material

consisted of 40.9% crystalline phase and 59.1% amorphous phase, indicating that the sample, while still predominantly amorphous, exhibited a significant increase in crystallinity after six months of storage (Figure 6).

DISCUSSION

The structural and chemical analysis of aluminum staples retrieved from used toothbrushes demonstrates that prolonged exposure to the oral environment induces progressive physicochemical changes. FTIR spectroscopy provided evidence of surface modifications, while XRD (where applicable) supports phase identification and crystallinity assessment.

At three months of use, the FTIR spectrum revealed strong O-H stretching vibrations, reflecting moisture adsorption and hydroxylation of the staple surface. The presence of C-H stretching peaks and carbonate-related bands indicated surface interactions with toothpaste residues and environmental contaminants. Distinct phosphate and silicate vibrations suggest deposition of inorganic components, most likely originating from abrasive agents commonly incorporated into dentifrices.

After six months of use, the FTIR spectra exhibited shifts and changes in the intensity of functional group bands. The broadening of the hydroxyl peak and persistence of phosphate/silicate bands indicate increased surface reactivity and deposition. The appearance of more pronounced carbonate features suggests ongoing interaction with oral fluids, leading to gradual incorporation of carbonate ions into the surface layer. These findings are consistent with the progressive chemical weathering and surface modification of metallic substrates in humid and chemically active environments.

The XRD analysis demonstrated clear changes in the structural composition of the material over the storage period. At three months, the sample exhibited a predominantly amorphous nature with 22.2% crystallinity and 77.8% amorphous content. By six months, however, crystallinity had increased substantially to 40.9%, while the amorphous fraction decreased to 59.1%. This progressive increase in crystalline domains suggests a gradual structural reorganization of the material during storage.

The appearance of sharp and intense peaks at 2θ values of 28.540° , 44.482° and 64.597° after six months highlights the development of ordered regions, indicating that the material becomes more structurally stable over time. The decrease in the amorphous fraction suggests reduced molecular disorder, which may influence properties such as solubility, stability and mechanical strength.

These findings align with the general behavior of semi-crystalline materials, where initially disordered regions slowly transform into more energetically favorable crystalline arrangements during storage. The transition toward higher crystallinity could enhance the stability of the material but may also reduce properties associated with the amorphous state, such as faster dissolution or higher reactivity. Overall, the XRD results confirm that the material undergoes significant structural evolution during storage, shifting from a largely amorphous to a more crystalline state with time.

Aluminum, though lightweight and cost-effective, displayed lower corrosion potential and higher reactivity. Its oxide layer was less stable, leading to potential long-term degradation under oral conditions. In contrast, nickel silver's passive film exhibited greater stability, supporting its durability in wet, acidic and fluctuating environments typical of the oral cavity.

The clinical relevance of these findings lies in reducing the risk of staple corrosion, preventing structural failures of toothbrush bristle tufts and minimizing exposure to metal ions that may leach into the oral cavity. The results strongly support nickel silver as a more reliable material for toothbrush staple applications.

FE-SEM, EDAX and Emap analysis confirmed the presence and uniform deposition of PHMB/TiO₂ onto the SS wire surface. Electrochemical tests revealed that the PHMB/TiO₂-coated SS wires exhibited a significantly lower corrosion rate (7.08×10^{-6} mm/year) and higher corrosion resistance (562466Ω) compared to bare SS [1].

The impact of solution treatment with both short and long-term aging on the Ti-6Al-4V (Grade 5) alloy's mechanical, wear and corrosion properties. Following a solution treatment that lasted 60 min at 960°C , the short-term aging (DHTS) treatment for 120 s at 550°C was conducted. Long-term aging (DHTL) procedures involve aging an alloy for 300 min at 550°C after the solution treatment. A ball-on-plate sliding wear testing equipment with Ti-6Al-4V alloy as the plate and an alumina ball as a pin was utilized. Open-circuit potential-time measurements and potentiodynamic polarization studies were employed to assess the corrosion potential behaviour in a 3.5% NaCl solution. The results reveal that the DHTS samples exhibit superior mechanical properties among the other samples. The hardness of the DHTS sample is 25.61% higher than that of the as-cast samples and 7.5% higher than that of the DHTL samples. The DHTS sample has a tensile strength of 23.26% greater and a tensile elongation of 36.32% lower than the as-cast alloy. The wear test findings show that the DHTS specimen exhibits the least wear. The DHTS specimen's wear rate is 3.4-folders lower than the As-Cast Alloy (ACT) and 1.6-folders inferior to the DHTL sample. The leading causes of the augmentation in mechanical and wear features of DHTS samples are the development of the α' -martensite phase upon quenching and the occurrence of a higher volume percentage of β -phase, which was maintained under DHTS conditions. The corrosion test reveals that the DHTS samples had greater corrosion resistance, as their icorr value was approximately 1.75-folders lower than the as-cast alloy and 1.3-folders lower than the DHTL sample [2].

The large volume of water produced alongside crude oil during extraction is a significant challenge in the oil and gas industry. Since crude oil emulsions can have a pH ranging from 2 to 13, inhibitors effective in acidic, basic and neutral media are essential for reducing the corrosion rate of transportation lines. This paper aims to elucidate the capability of corrosion inhibition of 1, 3-diphenyl prop-2-

en-1-one, a chalcone on mild steel corrosion in near acidic, neutral and near basic media using 1 N HCl, 3.5 % NaCl and 3.5% NaCl with 0.1 N NaOH made up to pH 8.5. The inhibitive competence of the inhibitor was determined by gravimetric, potentiodynamic polarization and electrochemical impedance spectroscopic studies. Nuclear magnetic resonance spectroscopy was used to characterize the carbon and hydrogen environment of the synthesized chalcones. The proposed inhibitor was found to give a good inhibition efficiency of 98.7% in acidic media and a reasonable decrease in corrosion rate in basic and neutral media. As the concentration of the inhibitor increases, the efficiency of inhibition increases, whereas, the efficiency decreases as the temperature increases. Potentiodynamic polarization confirmed that the inhibitor is of the mixed type. Impedance analysis explains the presence of an inhibitor as an adsorbed layer by a change in resistance and inhibition efficiency. The adsorption mechanism of the inhibitor on the mild steel surface is found to obey Langmuir's adsorption isotherm [3].

SEM Morphology of Neem Fiber

Field Emission Scanning Electron Microscopy is a characteristic tool to analyze the morphological parameters of the synthesized materials. Similarly, Energy Dispersive Spectroscopy is an important tool to investigate the elemental composition of the synthesized materials [4]. The neem fibers were assessed through FE-SEM and fiber-like integrated network structures were obtained. Flower-like spiky structures were noted on the fibers of impregnated neem fiber. Diameter of the moringa oleifera fiber is around 160 μm . On the surface of the fibers, spike-like structures indicate the morphology of neem leaf powder synthesized along PLA and the single impregnated neem fiber shows the surface of the fiber containing the rectangle and hexagonal structures. The uneven surface clearly displays unwanted contaminants such as hemicellulose, lignin residues and other non-cellulosic compounds. Furthermore, these pollutants facilitate the extraction of fibers from the matrix [1].

Inhibition effects of Irbesartan drug on mild steel corrosion in 1 M HCl and 0.5 M H₂SO₄ solutions have been investigated by Open Circuit Potential (OCP) curves, Tafel polarization curves, linear polarization curves and Electrochemical Impedance Spectroscopy (EIS) along with Cyclic Voltammetry (CV), UV-visible, FTIR and NMR spectroscopy techniques. Maximum corrosion inhibition of 94% and 83% have been achieved at 300 mg L⁻¹ Irbesartan concentration in 1 M HCl and 0.5 M H₂SO₄, respectively. Adsorption of Irbesartan on mild steel surface is studied by SEM and various isotherm models, which follows Langmuir isotherm. The effects of rise in temperature and acid concentration on the corrosion behavior of mild steel in both acid solutions are also studied by weight loss method. Corrosion inhibition by Irbesartan is explained on the basis of experimental results as well as frontier

molecular orbitals estimated by CV and UV-visible spectroscopic measurements [5].

The three parameters most frequently used for the corrosion evaluation are: the corrosion potential E_{corr} , the concrete resistivity ρ and the corrosion rate I_{corr} calculated from the polarization resistance R_p . In a real structure, the measurement of the three corrosion parameters allows the identification of the zones with high risk for damage. The principles of the use of the corrosion rate and the corrosion potential measurements for the evaluation of corrosion in reinforcement structures are described and current and future applications outlined [6].

The XRD analysis complements the FTIR results by identifying structural alterations in the aluminum staples. Over time, the formation of oxide phases or minor crystalline deposits on the staple surface may occur, reflecting corrosion processes and mineral accretion from toothpaste and saliva. Peak broadening in XRD patterns would further indicate surface disorder and possible amorphization due to prolonged exposure.

Together, the results highlight that aluminum staples in toothbrushes are not chemically inert during use. Instead, they undergo corrosion, hydroxylation and deposition of phosphate, carbonate and silicate species. These processes alter both the surface chemistry and structural stability of the staples, which may have implications for the long-term safety and durability of toothbrush designs incorporating metallic components.

CONCLUSIONS

Aluminum staples in toothbrushes undergo progressive structural degradation with usage time. XRD revealed a decrease in crystallinity and the emergence of aluminum oxide phases, while FTIR confirmed increasing surface hydroxylation and organic adsorption. Notably, Al₂O₃ and Al(OH)₃ phases become dominant after 3-6 months, suggesting increased corrosion susceptibility. These results support limiting aluminum staple usage within 3 months to maintain mechanical integrity and minimize oral contamination risks.

Ethical Approval

This was a prospective, two-arm, controlled clinical study conducted in the Department of Prosthodontics, Saveetha Dental College. Institutional ethical clearance was obtained and all participants gave informed consent.

REFERENCES

- [1] Raja, T. *et al.* "Study of Neem Fiber Composite Toothbrush-Latest Approach for the Prevention of Oral Disease." *Journal of Orofacial Sciences*, vol. 16, no. 2, July-December 2024, pp. 146-151. https://doi.org/10.4103/jofs.jofs_312_23.
- [2] Thirumal, K. *et al.* "Deposition of TiO₂/Polyhexamethylene Biguanide on Stainless Steel Wire for the Enhancement of Corrosion Resistance and Stability." *Current Nanoscience*, vol. 21, no. 5, 2025. <https://doi.org/10.2174/0115734137310115240812071132>.

- [3] Perumal, G. *et al.* “Comparative Analysis of Solution Treatment with Short and Long-Term Aging on Mechanical, Tribological, and Corrosion Potential of Ti-6Al-4V Alloy.” *Multiscale and Multidisciplinary Modeling, Experiments and Design*, vol. 8, 2025. <https://doi.org/10.1007/s41939-025-00759-6>.
- [4] Chenguttuvan, A. *et al.* “Preparation, Spectral Characterisation and Evaluation of Corrosion Inhibition Efficiency of 1,3-Diphenyl Prop-2-en-1-one.” *International Journal of Materials Research*, vol. 116, no. 7, 2025, pp. 570-583. <https://doi.org/10.1515/ijmr-2024-0168>.
- [5] Srivastava, M. *et al.* “Electrochemical Investigation of Irbesartan Drug Molecules as an Inhibitor of Mild Steel Corrosion in 1 M HCl and 0.5 M H₂SO₄ Solutions.” *Journal of Molecular Liquids*, 2017. <https://doi.org/10.1016/J.MOLLIQ.2017.04.017>.
- [6] Andrade, C. and I. Martínez. “Techniques for Measuring the Corrosion Rate (Polarization Resistance) and the Corrosion Potential of Reinforced Concrete Structures.” *Non-Destructive Testing Methods*, vol. 2, Woodhead Publishing Series in Civil and Structural Engineering, 2010, pp. 284-316. <https://doi.org/10.1533/9781845699604.2.284>.